

See discussions, stats, and author profiles for this publication at: <https://www.researchgate.net/publication/228879281>

# Simulations of Phospholipids Using a Coarse Grain Model

ARTICLE *in* THE JOURNAL OF PHYSICAL CHEMISTRY B · OCTOBER 2001

Impact Factor: 3.3 · DOI: 10.1021/jp011637n

---

CITATIONS

146

---

READS

58

6 AUTHORS, INCLUDING:



[John C Shelley](#)

Schrodinger

48 PUBLICATIONS 2,451 CITATIONS

SEE PROFILE



[Sanjoy Bandyopadhyay](#)

IIT Kharagpur

74 PUBLICATIONS 2,062 CITATIONS

SEE PROFILE



[Preston B Moore](#)

University of the Sciences in Philadelphia

73 PUBLICATIONS 2,790 CITATIONS

SEE PROFILE

# Simulations of Phospholipids Using a Coarse Grain Model

John C. Shelley,<sup>\*,†,‡</sup> Mee Y. Shelley,<sup>‡,§</sup> Robert C. Reeder,<sup>†</sup> Sanjoy Bandyopadhyay,<sup>||</sup>  
Preston B. Moore,<sup>||</sup> and Michael L. Klein<sup>||</sup>

*The Procter & Gamble Company, Miami Valley Laboratories, P.O. Box 538707, Cincinnati, Ohio 45253-8707,  
Department of Chemistry and Biochemistry, Miami University, Oxford, Ohio 45056, and  
Center for Molecular Modeling, Department of Chemistry, University of Pennsylvania,  
Philadelphia, Pennsylvania 19104-6323*

*Received: May 1, 2001; In Final Form: July 6, 2001*

A computationally efficient coarse grain model designed to closely mimic specific phospholipids is used to study a number of phospholipid systems to demonstrate its strengths and weaknesses. A study of a membrane containing an anesthetic, halothane, illustrates the shortcomings of this model in treating systems without extensive parametrization. In contrast, the power of the model is demonstrated by its ability to successfully simulate the self-assembly of two phospholipid phases from random initial configurations: a lamellar phase and a reverse hexagonal phase in a ternary system containing water, a hydrocarbon, and a phospholipid. The aqueous columns in the reverse hexagonal phase tend to adopt polygonal cross sections and the local structure of phospholipids is still bilayer-like. Molecular dynamics was found to be much more efficient at simulating self-assembly in the current systems than Monte Carlo.

## 1. Introduction

Collective molecular behaviors in general are currently of great interest. Biological systems exhibit many such behaviors. In particular, processes involving the phospholipids including membrane fusion<sup>1–6</sup> and the effect of phospholipids on protein interactions<sup>7–10</sup> are the focus of recent studies. Developing an understanding of the complexities of collective molecular behavior presents a challenge that computer simulation in conjunction with experiment may be able to meet.

Atomic simulation has developed to the extent that it is possible to accurately mimic phospholipid membranes.<sup>11–16</sup> Unfortunately, current algorithms and computer power limit such studies to length and time scales that put much of the collective phenomena described above out of reach. The use of coarse grain (CG) models can partially alleviate this problem because they use dramatically less computer time to simulate phenomena. Generalized CG models have been applied to study phospholipid bilayer behavior.<sup>17–19</sup>

We recently introduced a CG model that is designed to accurately mimic a particular phospholipid, dimyristoylphosphatidylcholine (DMPC).<sup>20</sup> This CG model is significantly more efficient at modeling phospholipids than atomistic models. The current paper explores the limits of this model and demonstrates how it can be used to study phospholipid systems, especially to learn about collective phenomena including the self-assembly process.

In the following section, we briefly describe the nature of the model and how it was adapted for molecular dynamics simulations. Next we describe three trial applications of this model: solubilization of an anesthetic in a phospholipid bilayer

and the formation of lamellar and reverse hexagonal liquid crystalline phases of phospholipids. Then we will summarize what our results mean in terms of the capabilities and limitations of the current approach.

## 2. Methodology

This model uses simplified representations for water, alkanes, and phospholipids. For each type of molecule we constructed a model that mimics some key physical or structural features known from experiment or atomistic simulations.<sup>21</sup> The model and its development are described in detail in our earlier paper.<sup>20</sup> Briefly, triplets of water molecules are represented by single spherical sites. Triplets of carbon atoms in hydrocarbon chains and their accompanying hydrogen atoms are also represented by single spherical sites. The hydrocarbon sites are linked together to form chains using stretching and bending potentials.

The CG model for DMPC is depicted in Figure 1. Single spherically symmetric sites were used to represent each of the choline (CH), phosphate (PH), glycerol backbone (GL, namely CH<sub>2</sub>–CH–CH<sub>2</sub>), and ester groups (O<sub>2</sub>CCH<sub>2</sub>–, E1, and E2). The hydrocarbon chains were modeled using the alkane model described above. The CH and PH groups carried charges of  $+e$  and  $-e$ , respectively, and a dielectric constant of 78 was used. “Tinfoil” Ewald periodic boundary conditions were used to treat the electrostatic interactions. The van der Waals interactions were truncated at 15 Å, while the real-space portions of the electrostatic interactions were truncated at distances between 15 and 22.5 Å depending on the system being studied. An analogous model for DHPC was constructed by including an additional SM site (representing (CH<sub>2</sub>)<sub>3</sub>) in the hydrocarbon chains. The DMPC model semiquantitatively reproduces the atomistic density profiles<sup>21</sup> of the various components perpendicular to the phospholipid bilayer.<sup>20</sup> This model erroneously generates high pressures of about 1 kbar. The cause of this problem is being investigated and will be eliminated, if possible, in future work.

\* Corresponding author. E-mail: jshelley@schrodinger.com.

† Procter & Gamble.

‡ Current address: Schrödinger Inc., 1500 S. W. First Ave., Suite 1180, Portland, OR 97201.

§ Miami University.

|| University of Pennsylvania.

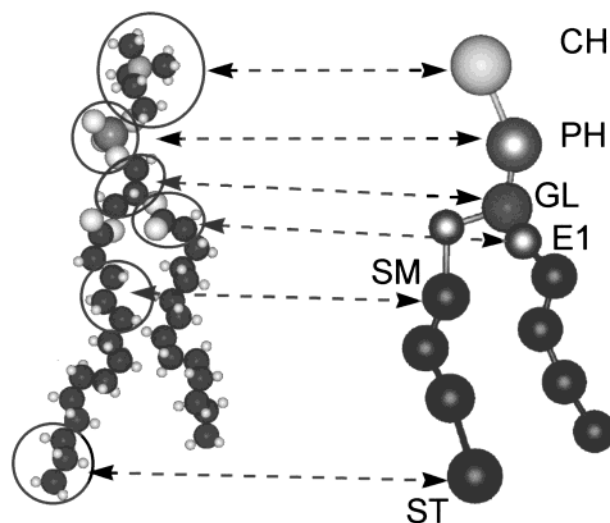


**Figure 1.** Atomistic (left) and coarse grain (right) representations of dimyristoylphosphatidylcholine (DMPC). Single spherically symmetric sites are used to represent each of the choline (CH), phosphate (PH), glycerol backbone (GL, namely  $\text{CH}_2\text{--CH--CH}_2$ ), and ester groups (E1 and E2,  $\text{O}_2\text{CCH}_2$ , collectively referred to as E). The alkane portions of the DMPC molecules consist of sites representing triplets of carbon atoms and their accompanying hydrogen atoms.  $(\text{CH}_2)_3$  is referred to as an SM site while  $(\text{CH}_2)_2\text{--CH}_3$  is referred to as an ST site. SM and ST sites are collectively referred to as S.

We employed Monte Carlo (MC) simulations with changes involving single site and whole molecule moves, the magnitude of which was systematically adjusted to maintain an acceptance rate of 25%. Unlike MC studies of atomistic systems, we did not find that sampling internal coordinates had a significant effect on computational efficiency using this model, likely due to the softness of the potentials employed. In our earlier paper<sup>20</sup> we found that MC simulations of self-assembly using this model often produce structures containing defects.

In some studies we employed molecular dynamics (MD) simulations using the program "mike" in a manner completely consistent with that for the MC simulations. The MD simulations were conducted in the canonical ensemble using Nosé–Hoover chains<sup>22,23</sup> of length 4. Multiple time step molecular dynamics was implemented using a three-stage RESPA integration of the equations of motion.<sup>23</sup> The shortest steps, 1 fs, were used for bond length and angle integration while the intermediate length steps, 2 fs were used for nonbonded interactions less than 11 Å, and the long steps, 40 fs, were used for nonbonded interactions between 11 Å and the cutoff. The cutoff for the van der Waals potentials was set at 15 Å, while that for the real-space part of the Ewald calculations was 22.9 Å.

The tabulated potentials, used to describe interactions among the CH, PH, GL, and E sites, as developed for the MC simulations, are too rough to employ in MD studies. These potentials were smoothed for distances larger than the steep repulsive wall by differentiating them three times, replacing the value of the derivative by the central average of five adjacent points, and then integrating back to obtain the potential and forces. Some additional manual adjustments of the raw potentials were used, particularly where the smoothing was turned on at small distances. Figure 2 compares the initial MC and smoothed potentials for the case most strongly affected by smoothing, the CH–PH potential (a), and a more typical potential, PH–GL (b). All of the smoothed potentials are depicted in Figure 3. A complete compilation of the potentials including the tabulated potentials is available from <ftp://ftp.schrodinger.com/support/jshelley/JP011637N.tar.gz>.

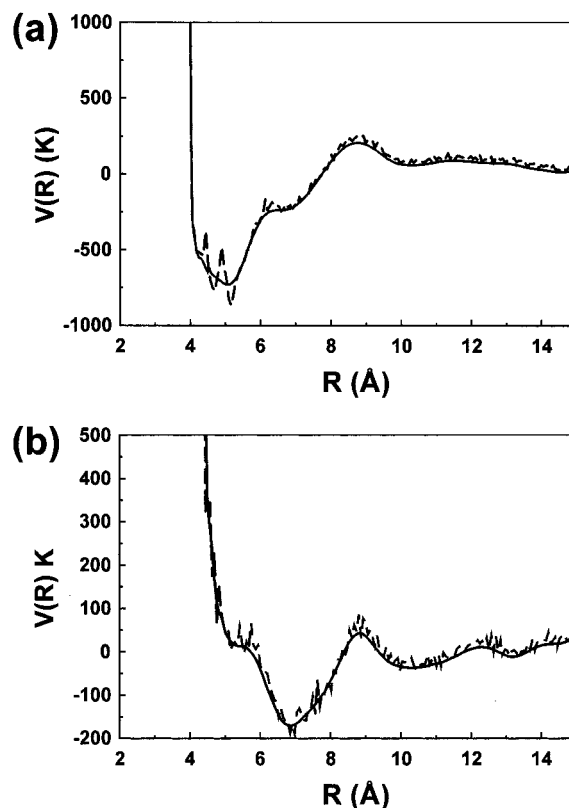


**Figure 2.** Comparisons of smoothed (solid) and fitted pair potentials (dashed) for CH–PH (a) and PH–GL (b). The CH–PH potential was the potential most strongly affected by smoothing, while the PH–GL potential is representative of the changes introduced by smoothing for most tabulated potentials.

### 3. Applications

Three studies were performed: one study of the anesthetic halothane in a DMPC bilayer and two studies of self-assembly of phospholipid liquid-crystalline phases, a lamellar phase and a reverse hexagonal phase.

**A. Anesthetics.** Recently, an atomistic simulation of halothane in a dipalmitoylphosphatidylcholine (DPPC) bilayer was conducted.<sup>24</sup> This study provides an opportunity to test the adaptability of the current CG model without utilizing extensive raw data from atomistic studies to develop a CG model for a new component, the halothane. For the current CG study we chose to use DMPC. A single site, referred to as an H, was used to represent the halothane, a choice justified by the fact that the orientational distributions of halothane molecules within the bilayer were fairly isotropic.<sup>24</sup>

In the present study, we describe interactions among halothane molecules by a Lennard-Jones 6–4 potential

$$V(r_{ij}) = \frac{15}{4} \epsilon_{\alpha\beta} \left\{ \left( \frac{\sigma_{\alpha\beta}}{r_{ij}} \right)^6 - \left( \frac{\sigma_{\alpha\beta}}{r_{ij}} \right)^4 \right\}$$

where  $r_{ij}$  is the distance between sites  $i$  and  $j$ .  $\epsilon_{\alpha\beta}$ , the depth of the potential well, and  $\sigma_{\alpha\beta}$ , the characteristic distance for the interaction, are constants determined by the types of interacting sites,  $\alpha$  and  $\beta$ . The experimental density (1.3697 g/mol at 20 °C<sup>25</sup>) and boiling point (50.2 °C<sup>25</sup>) of halothane were used to fix  $\epsilon_{\text{HH}}$  and  $\sigma_{\text{HH}}$  in a manner similar to that used to parametrize the model for the water sites W.<sup>20</sup>

A Lennard-Jones 6–4 potential was used to represent the halothane–water interaction.  $\sigma_{\text{HW}}$  was the average of the water and halothane interactions.  $\epsilon_{\text{HW}}$  was set by matching the

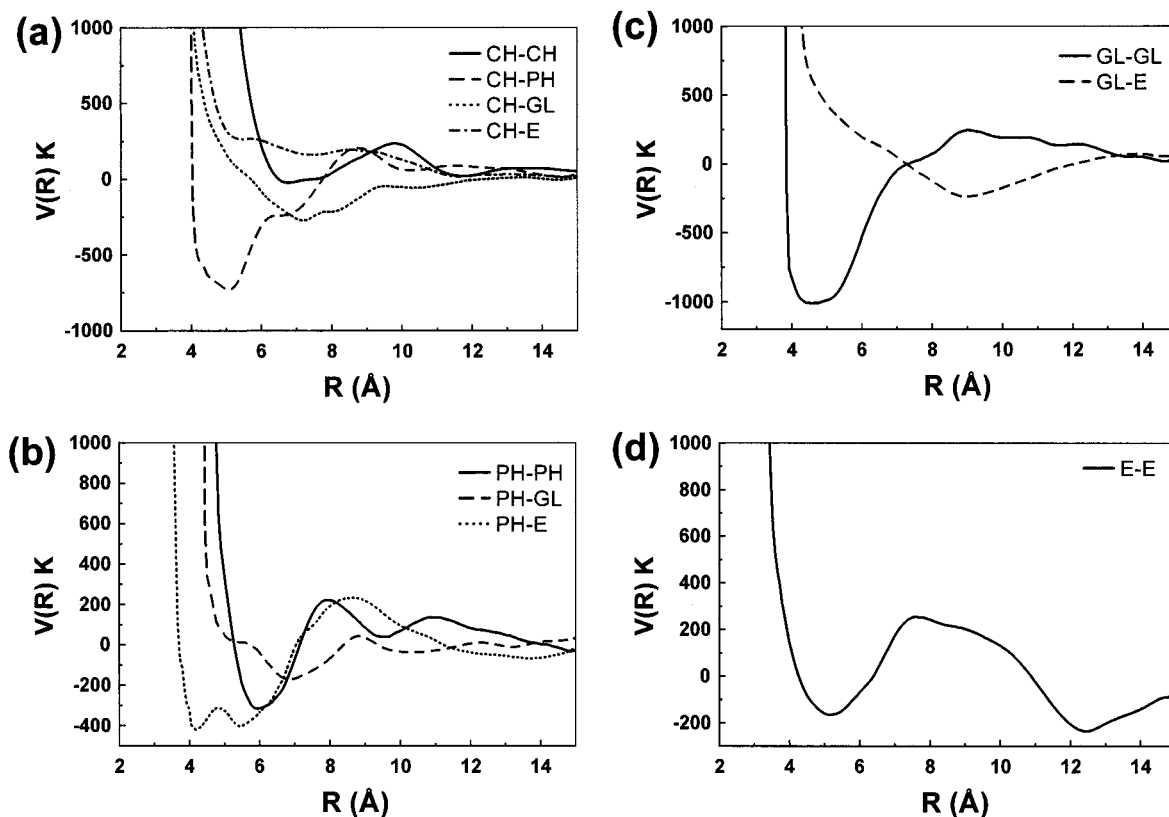


Figure 3. Smoothed potentials among the CH, PH, GL, and E groups.

TABLE 1: Parameters for Nonbonded Potentials Involving Halothane Sites

sites	type <sup>a</sup>	$\sigma$ (Å)	$\epsilon$ (K)
W-H	LJ64	5.154	125.5
SM-H	LJ64	5.04275	150.0000
ST-H	LJ64	5.1665	150.0000
E-H	LJ96	5.67	194.4362
PH-H	LJ96	5.56	194.4362
GL-H	LJ96	5.36	194.4362
CH-H	LJ96	7.36	250.0
H-H	LJ64	5.728	183.7

<sup>a</sup> These parameters are for Lennard-Jones 9–6 (LJ96) or 6–4 (LJ64) nonbonded potential forms.

solubility of halothane in water as follows. Grand canonical Monte Carlo simulations of halothane in water, represented by W sites, were conducted, with the chemical potentials fixed at the values of the bulk liquids.  $\epsilon_{\text{HW}}$  was adjusted until the solubility of halothane matched experiment (0.345 wt %<sup>25</sup>). See Table 1 for the H–W and H–H potential parameters.

There is not much information to go on to establish initial estimates for the membrane–halothane interaction potential parameters. Lennard-Jones 6–4 potentials were used for the S–H potentials. Lennard-Jones 9–6 potentials

$$V(r_{ij}) = \frac{15}{4} \epsilon_{\alpha\beta} \left\{ \left( \frac{\sigma_{\alpha\beta}}{r_{ij}} \right)^9 - \left( \frac{\sigma_{\alpha\beta}}{r_{ij}} \right)^6 \right\}$$

were used for the CH, PH, GL, and E interactions with halothane. The  $\sigma_{\alpha\beta}$  values for the various phospholipid–halothane interactions were set at roughly the average of the corresponding  $\sigma_{\alpha\beta}$  for the pure interactions. Initially the  $\epsilon_{\alpha\beta}$  for these interactions was arbitrarily chosen to be 194.4 K for all halothane–phospholipid site–site interactions.

For the current study, we chose to introduce the halothane molecules into a preassembled DMPC bilayer used in our earlier

work.<sup>20</sup> We maintained the same 2:1 ratio of the phospholipid to halothane molecules used in the atomistic simulation.<sup>24</sup> The resulting system contained 428 W sites, 50 DMPC molecules, and 25 H sites. This system had less water than the atomistic study. The box shape was orthorhombic with  $|a| = |b| = 42.4$  Å, while  $|c| = 54.17$  Å, yielding the same surface area per phospholipid, 72 Å<sup>2</sup>, as found in the atomistic study.<sup>24</sup> The simulation was conducted at 303.15 K as opposed to 323.15 K because the phospholipids in the current study contain shorter hydrocarbon chains.

The system was equilibrated for 200 000 MC passes using about 1 CPU day of SGI R12000 processor time. Significant diffusion of the halothane occurred during this simulation. A subsequent production run 200 000 MC passes long was used to estimate the halothane distribution perpendicular to the surface of the bilayer. This distribution was qualitatively different than that found in the atomistic studies, indicating that our initial CG model was not well-constructed. After several adjustments of  $\epsilon_{\text{S-H}}$  and  $\epsilon_{\text{CH-H}}$  and subsequent 200 000 pass simulations, the distribution of the halothane perpendicular to the membrane was brought into qualitative agreement with the atomistic study (See Figure 4). Table 1 lists the van der Waals parameters used to obtain the best distribution, and Figure 5 is an image of the final configuration obtained from the simulation carried out using these parameters.

This study indicates that the current methodology and level of experience cannot provide predictive models in the absence of careful parametrization using extensive data. On the other hand, adjusting the parameters to obtain reasonable agreement with existing atomistic data was not difficult. The resulting model, while still not having the accuracy of the atomistic one, is significantly faster, thus providing the opportunity to explore some issues regarding anesthetics mechanisms on longer length and time scales.



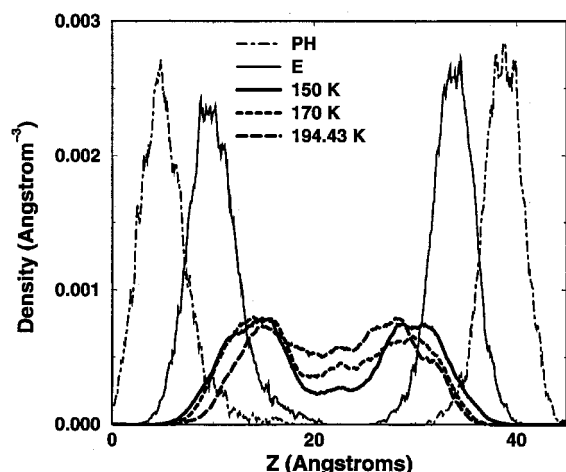


**Figure 4.** Density profiles perpendicular to the bilayer for the coarse grain simulation containing halothane. Curves are given for PH, E, and three choices of the well depth for the H-S interaction potentials (labeled 150, 170, and 194.43 K). The results for the potential with well depths of 150 K resemble those obtained from an atomistic study.<sup>24</sup> See Table 1 for the other potential parameters involving H sites.

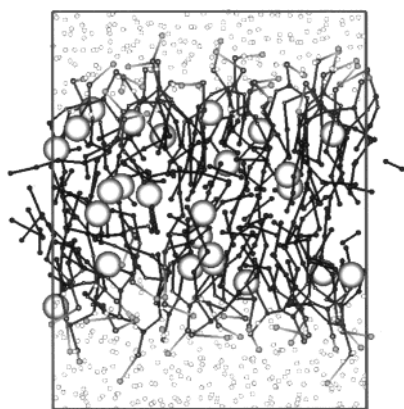


**Figure 5.** Final configuration from the simulation of the phospholipid bilayer containing halothane. All sites are represented using a ball-and-stick representation except for the halothane, for which a space-filling representation is used.

**B. Self-Assembly of a Phospholipid Bilayer.** As a test of the model and its efficiency, a simulation of the self-assembly of a system containing 428 W sites and 50 DMPC molecules at 303.15 K into a bilayer structure was carried out. The unit cell was orthorhombic with  $|a| = |b| = 39.375$  Å and  $|c| = 58.98$  Å. This study was conducted using a Monte Carlo simulation and was partially described in ref 20. Briefly, the initial configuration was constructed by first randomly inserting DMPC molecules and then randomly inserting the W sites. Only the insertions which resulted in molecules that were essentially on top of each other were rejected during this process. The resulting configuration is depicted in Figure 6a. Then the system was simulated using standard canonical Monte Carlo moves for 1 050 000 passes (where a pass was defined as 1 move per site). The simulation took 11 days on a Silicon Graphics Origin 200 with a 250 MHz R12000 MIPS processor. Configurations from every 150 000 passes are depicted in Figure 6 (panels a–j).

The DMPC self-assembles into a bilayer structure. However, two defects remain: a group of four phospholipid headgroups remains in the core of the bilayer, and a hydrocarbon chain from one DMPC molecule extends outside the bilayer. Other simulations, including one with a larger cubic box (58.98 Å on a side containing 112 DMPC and 960 W) gave similar results. While

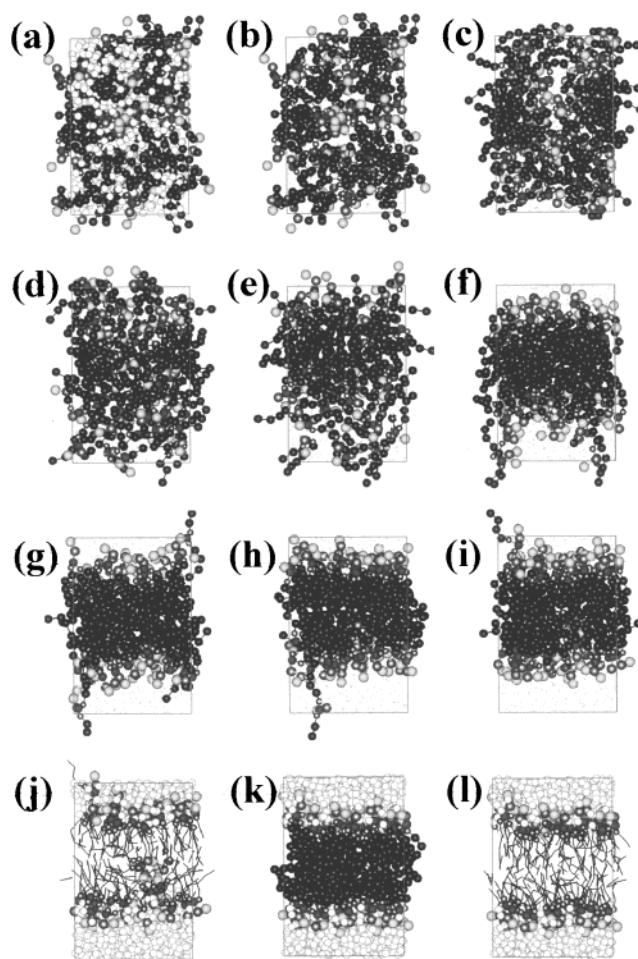


**Figure 6.** Images from a simulation of the assembly of a bilayer starting from a random configuration. (a) is an image of the initial configuration using space filling representation. (b)–(i) are images of the system starting from the initial state and at intervals of 150 000 Monte Carlo passes. In these images the water is displayed using small radii to facilitate viewing the phospholipids. In (j) all components of the system are displayed as space filling except for the hydrocarbon chains, which are displayed using a stick representation. In (j) there are two defects: one in which a group of four phospholipid headgroups remain in the core of the bilayer, and the other in which a hydrocarbon chain from one DMPC molecule extends outside the bilayer within an otherwise well-assembled bilayer. A molecular dynamics simulation was started from the configuration depicted in (j), and very quickly the defects healed, leaving a well-formed bilayer depicted in (k) (space filling, and (l) (space filling except that the hydrocarbon chains are displayed using a stick representation).

the general assembly of the bilayer is encouraging, the presence of defects is disappointing.

Evidence exists that maintaining consistency with hydrodynamics, especially conservation of momentum, in simulations leads to more efficient modeling of collective organization.<sup>26–28</sup> The current Monte Carlo simulations do not track or conserve momentum. Consequently, we decided to switch to using a molecular dynamics simulation. Within 6 ns (2 CPU days) all of the defects healed and a defect-free bilayer resulted as depicted in Figure 6k,l. All the defects in all self-assembly studies of phospholipid bilayers disappeared in a similar manner. A test MC study conducted using the same smoothed potentials used in the MD simulations did not heal the defects within 200 000 passes.

**C. Self-Assembly of Phospholipids in a Reverse Hexagonal Phase.** Reverse hexagonal phases are of particular interest in understanding a number of phenomena including membrane

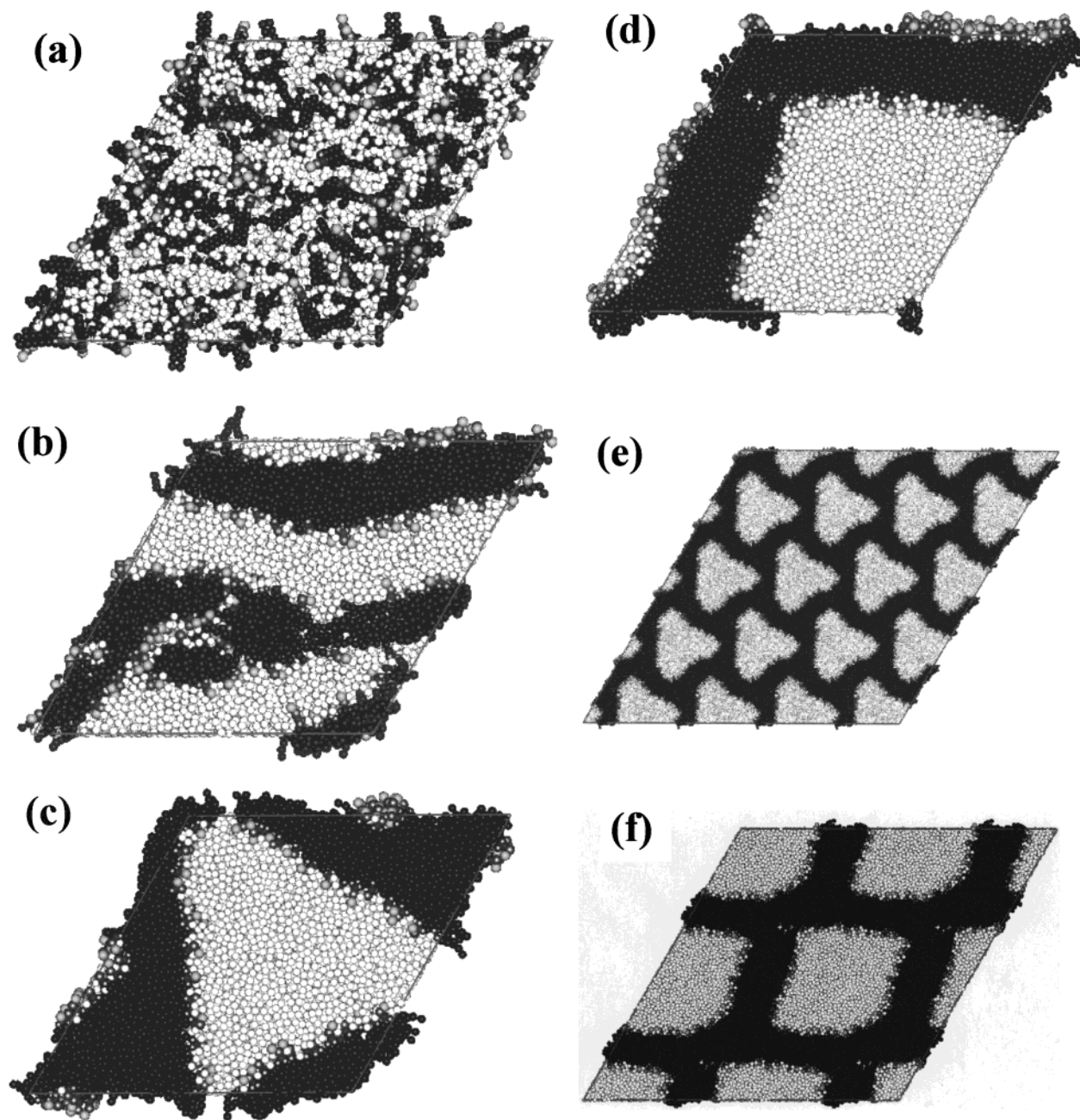


**Figure 7.** Images of reverse hexagonal simulations containing a single unit cell. The initial and final configurations for the Monte Carlo portion of the study are depicted in (a) and (b), respectively. While the DHPC has associated locally, the aggregates are irregular and small. The final structure from the first and second molecular dynamics simulations of this system are depicted in (c) and (d). (e) and (f) are  $4 \times 4$  and  $2 \times 2$  replications of the systems from (c) and (d), respectively. The collective organization exhibited at the end of the molecular dynamics simulation is far more developed than that obtained from Monte Carlo simulations requiring similar amounts of computer time.

fusion.<sup>2,5</sup> Experimental results exist concerning the formation of a reverse hexagonal phase in systems containing phosphatidylcholine based lipids, alkanes, and water.<sup>2</sup> The current model without additional parameters can be used to study such a system. Simulation of the formation of hexagonal phases is believed to be more challenging than the related lamellar phases<sup>27</sup> and provides us with a tough test of the quality and efficiency of the current model.

In the current model, hydrocarbons are represented by sites containing three carbon atoms and the hydrogen atoms bonded to them. This restriction means that we must study systems containing molecules that are slightly different than those employed in the experiment.<sup>2</sup> We chose to use diheptadecanoylphosphatidylcholine (DHPC) and nonane since they most closely resemble the molecules used in the experiment that had

the highest tendencies to form reverse hexagonal phases. Experimental systems containing 24 C atoms from alkanes per phospholipid and roughly 50 wt % water at a temperature of 55 °C had a strong tendency to form reverse hexagonal phases. The simulated system, chosen to mimic these conditions, consisted of 7530 W sites (50.5 wt % water), 369 DHPC molecules (33.8 wt %), and 984 nonane molecules (15.7 wt %, 24 C/DHPC) in a rhombohedral box with  $|a| = |b| = 176.6$  Å, while  $|c| = 50.0$  Å and  $\alpha = \beta = 90.0^\circ$  and  $\gamma = 60^\circ$ . This system contains more than 16 000 sites. While the system is fairly large by atomistic simulation standards, it is still only barely large enough to contain roughly what we estimate to be one unit cell (and thus one inverse column of phospholipids) based upon information from the experiments.<sup>2</sup> The initial



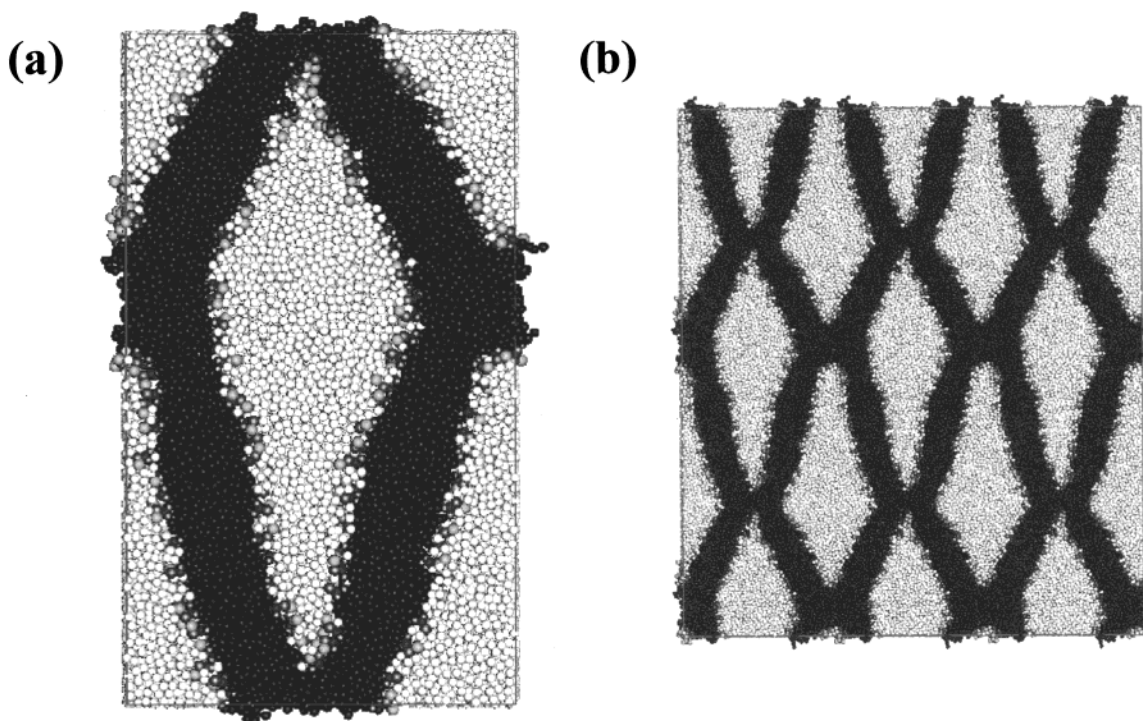


**Figure 8.** Images of the final configuration of the larger reverse hexagonal simulation. (a) depicts the simulated cell which contains two unit cells, while (b) depicts a  $2 \times 3$  replication of the simulated system.

configuration (see Figure 7a) was generated in a random manner analogous to that used for the bilayer self-assembly studies.

As for the bilayer self-assembly, an extensive simulation employing simple MC methods failed to assemble the system into a reasonable configuration. In fact, after simulating at 55 °C for 180 000 MC passes requiring 4 months of CPU time on an SGI R12000 processor, the system lacked large-scale organization (see Figure 7b). We then switched to simulating this system using molecular dynamics in a manner completely analogous to that used for the bilayer MD simulation. Collective organization of the system was noticeable within 1.2 ns (30 000 time steps, about 2 weeks of CPU time), and after 10.3 ns (258 000 time steps) the columnar structure depicted in Figure 7c was produced.

As an additional check, MD simulation was carried out starting from a configuration generated much earlier in the MC run (50 000 passes). This system also assembled within 4 ns into a single column as depicted in Figure 7d. Note, however, that the columns from these two studies have different shapes. Since the box shape for systems which contain only one unit cell is expected to influence the results, we performed another simulation on a system with an orthorhombic box with  $|a| = 176.6 \text{ \AA}$ ,  $|b| = 305.9 \text{ \AA}$ , and  $|c| = 50.0 \text{ \AA}$ , which is large enough to contain two unit cells. After simulating for 2.6 ns (8 weeks of CPU time), this system assembled in a structure containing two columns with rhombohedral cross sections, as did the second study containing only one unit cell (See Figure 8).

This final study presents an opportunity to learn about the self-assembly process for this phase. Figure 9 shows the initial and final (47 000 passes) images of the MC portion of the simulation. While some local aggregation of the phospholipids is noticeable in the final image, no large-scale organization is evident. Figure 10 shows images at 160 ps intervals for the MD portion of the simulation. Collective organization rapidly takes place during this 2.6 ns simulation. By around 400 ps essentially no monomers reside outside aggregates and the aggregates are progressively joining together to form two large extended

structures. These structures thicken and become smoother, forming well-defined bilayers with a few tenuous bridges between them. At 1.2 ns two of these bridges become substantial and the final topology of the system is established. For the remainder of the simulation there are local fluctuations in the thickness of the bilayers. Note that the MD portion of the simulation used roughly as much CPU time as the MC portion, illustrating the much greater efficiency of MD for assembling this phase.

Since the systems that were simulated contain only one or two unit cells and have box sizes consistent with the estimated unit cell size, the above results are not conclusive. However, the fact that all three studies gave results consistent with our estimate of the unit cell size based upon experimental results<sup>2</sup> is encouraging.

The simulations always gave columns of water that have triangular or rhombohedral cross sections rather than round. Using the composition of the experimental systems, it is possible to estimate the surface area per phospholipid assuming that the columns of water are perfectly round. Such a calculation yields a surface area of approximately  $57 \text{ \AA}^2$  per phospholipid, which is less than that obtained from experiment for DPPC liquid crystalline bilayers at 323.15 K,<sup>29</sup> namely  $62.9 \text{ \AA}^2$ . This comparison suggests that it is possible that the columns of surfactant may need to roughen in order to accommodate the amount of phospholipid present. In addition, an examination of the replicated versions of simulated systems (Figures 7e,f and 8b) suggests a tendency toward retaining a bilayer-like local structure where the two halves of the bilayer come from different columns. Perhaps the system is attempting to retain some bilayer character in this phase. Such a tendency could lead to columns with sides that are polygon-like.

We suspect that the speed of self-assembly in the current dynamic simulations is faster than that for the corresponding real systems. Possible reasons for this include the following:

1. The soft, smoothened potentials eliminate many local minima in the potential energy surface.

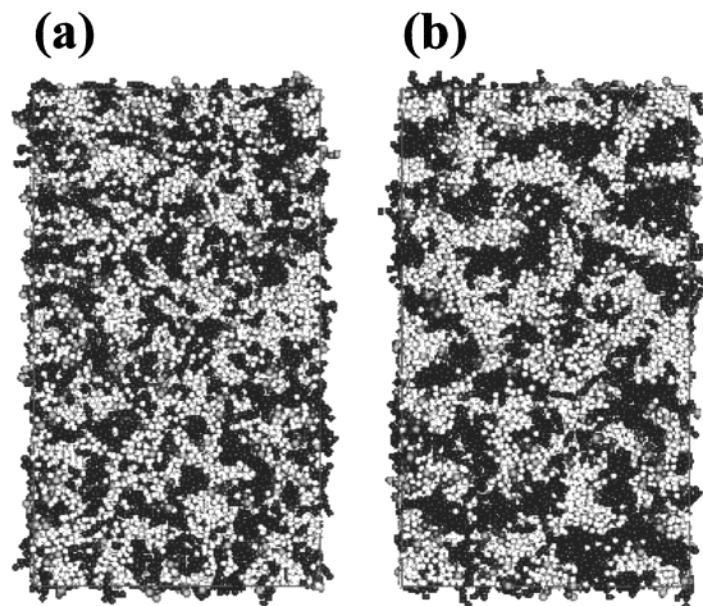


**Figure 9.** Initial and final configurations of the MC portion of a simulation of the reverse hexagonal phase that was large enough to contain two unit cells. Note that only local aggregation of the phospholipid occurs during this period.

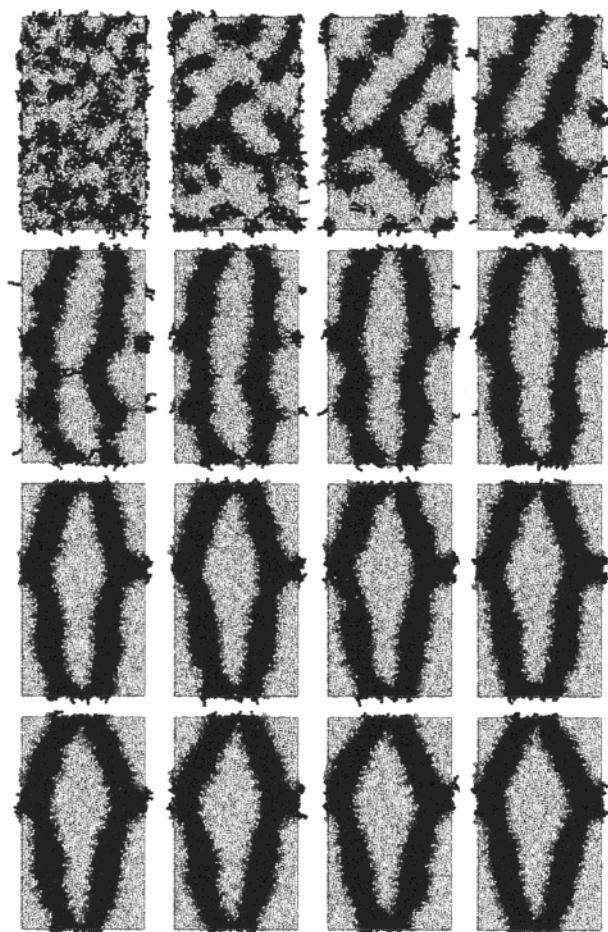


**Figure 10.** Configurations from 160 ps intervals during MD portion of a simulation of the reverse hexagonal phase, starting from the upper left and proceeding across each row. Structural development proceeds rapidly through stages of local aggregation, agglomeration of aggregates into bilayers, and bridging of the bilayers to form a reverse hexagonal phase.

2. Models containing fewer independent sites encourage collective motion.

3. The systems studied involve only one or two unit cells providing a feedback mechanism for self-assembly.

While one might suggest that the high pressures produced by the current model could enhance the rate of self-assembly, our experience with related systems that are not under such pressures suggests otherwise.

#### 4. Summary

A CG model for phospholipids, which semiquantitatively reproduces the density profile of an aqueous DMPC bilayer,<sup>20</sup> has been applied to several phospholipid systems. Simulating a simple solute halothane in a bilayer showed that these models cannot be truly predictive in the absence of sufficient data for careful parametrization with the current level of experience. On the other hand, with such data the model could be readily adapted to reproduce the results of atomistic simulations. In such circumstances the CG model may still have a role to play in extending, in a complementary way, the range of phenomena addressable by simulations.

The model has been used to simulate the self-assembly of a DMPC bilayer from a thoroughly mixed initial state. Finally, the CG model was used to simulate the formation of a reverse columnar phase in a system composed of phospholipids, alkanes, and water, a particularly difficult problem. The columns that form in this phase do not appear to be cylindrical but are roughly polygonal, and the phospholipids tend to locally adopt bilayer-like arrangements. The self-assembly process for this phase initially proceeds through local aggregation to an intermediate stage involving bilayers which join together to form the reverse hexagonal structure. It should be possible to test these predictions using experimental techniques such as neutron or X-ray scattering.

Clearly, the current CG model is sufficiently accurate to study a range of phenomena at a level of efficiency that uses orders of magnitude less computer processor time than atomistic models. Monte Carlo, a nonhydrodynamic simulation approach, was not able to produce defect-free structures in long simulations consistent with other published studies.<sup>27,28</sup> In contrast, molecular dynamics implemented in a manner consistent with hydrodynamics readily produced such structures. These results



suggest that molecular dynamics is more efficient for modeling collective motions within dense molecular systems.

The current CG model conceptually lies between atomistic models and those employed in dissipative particle dynamics (DPD). The models employed in DPD studies are typically predominantly repulsive and soft in part due to the internal flexibility represented by single sites. As a result, DPD studies of liquids are nearly always conducted under high pressures at constant volume. In developing the current model, we chose to set aside the issue of what pressure to use and explore the potential of carefully parametrized CG models to study structured fluids, of which phospholipids are among the most important. The pressure that this model produces at the right densities is high at 1 kbar. The current model has not been tested at constant pressure. We are currently striving to adapt this model to perform well under a constant pressure of 1 atm.

We envision that this and related models could be used to imitate a wide range of phenomena in phospholipid systems such as self-assembly (particularly of larger systems containing multiple bilayers), fluctuations of the bilayer, lateral partitioning of phospholipids, and membrane fusion. We have constructed similar models for surfactant systems.<sup>30</sup> The CG models could be used in conjunction with atomistic models to take advantage of the strengths of both approaches. For instance, one could simulate a key region of a system using atomistic models and use CG models to simulate regions of the system that surround this region.

The current model has a number of limitations as noted in ref 20. However, it should serve as an example for what is possible with coarse grain models which have been parametrized to mimic specific chemical components. Additional application and testing of this model should help further elucidate its strengths and limitations.

**Acknowledgment.** We gratefully acknowledge useful discussions with Robert Corkery, Charlie Eads, Gren Patey, and Dave Siegel.

## References and Notes

- (1) Marsh, D. *Chem. Phys. Lipids* **1991**, 57, 109.
- (2) Sjölund, M.; Rilfors, L.; Lindholm, G. *Biochemistry* **1989**, 28, 1323.
- (3) May, S.; Ben-Shaul, A. *Biophys. J.* **1999**, 76, 751.
- (4) Siegel, D. P.; Epand, R. M. *Biophys. J.* **1997**, 73, 3089.
- (5) Siegel, D. P. *Biophys. J.* **1999**, 76, 291.
- (6) Jahn, R.; Südhof, T. C. *Annu. Rev. Biochem.* **1999**, 68, 863.
- (7) de Kruljff, B. *Nature* **1997**, 386, 129.
- (8) Gil, T.; Ipsen, J. H.; Mouritsen, O. G.; Sabra, M. C.; Sperotto, M. M.; Zuckermann, M. J. *Biochim. Biophys. Acta* **1998**, 1376, 245.
- (9) Mouritsen, O. G. *Curr. Opin. Colloid Interface Sci.* **1998**, 3, 78.
- (10) Landau, E. M.; Rosenbusch, J. P. *Proc. Natl. Acad. Sci., U.S.A.* **1996**, 93, 14532.
- (11) Feller, S. E.; Pastor, R. W. *J. Chem. Phys.* **1999**, 111, 1281.
- (12) Essman, U.; Berkowitz, M. L. *Biophys. J.* **1999**, 76, 2081.
- (13) Armen, R. S.; Uitto, O. D.; Feller, S. E. *Biophys. J.* **1998**, 75, 734.
- (14) Tobias, D. J.; Tu, K.; Klein, M. L. *Curr. Opin. Colloid Interface Sci.* **1997**, 2, 15.
- (15) Tieleman, D. P.; Berendsen, H. J. C. *J. Chem. Phys.* **1996**, 105, 4871.
- (16) Tu, K.; Klein, M. L.; Tobias, D. J. *Biophys. J.* **1998**, 75, 2147.
- (17) Goetz, R.; Lipowsky, R. *J. Chem. Phys.* **1998**, 108, 7397.
- (18) Weikl, T. R.; Netz, R. R.; Lipowsky, R. *Phys. Rev. E* **2000**, 62, R45.
- (19) Goetz, R.; Gompper, G.; Lipowsky, R. *Phys. Rev. Lett.* **2000**, 82, 221.
- (20) Shelley, J. C.; Shelley, M. Y.; Reeder, R. C.; Bandyopadhyay, S.; Klein, M. L. *J. Phys. Chem. B* **2001**, 105, 4464.
- (21) Bandyopadhyay, S.; Shelley, J. C.; Klein, M. L. *J. Phys. Chem. B* **2001**, 105, 5979.
- (22) Frenkel, D.; Smit, B. *Understanding molecular simulation*; Academic Press Inc.: San Diego, 1996.
- (23) Tuckerman, M. E.; Martyna, G. J. *J. Phys. Chem. B* **2000**, 104, 159.
- (24) Koubi, L.; Tarek, M.; Klein, M. L.; Scharf, D. *Biophys. J.* **2000**, 78, 800.
- (25) *The Merck Index*; Budavari, S.; O'Neil, M. J.; Smith, A.; Heckelman, P. E.; Kinneary, J. F., Eds.; Merck & Co.: Whitehouse Station, NJ, 1996.
- (26) Patey, G. N. Private discussions.
- (27) Groot, R. D.; Madden, T. J.; Tildesley, D. J. *J. Chem. Phys.* **1999**, 110, 9739.
- (28) Maurits, N. M.; Zvelindovsky, A. V.; Sevink, G. J. A.; van Vlimmeren, B. A. C.; Fraaije, J. G. E. M. *J. Chem. Phys.* **1998**, 108, 9150.
- (29) Nagle, J. F.; Zhang, R.; Tristram-Nagle, S.; Sun, W. J.; Petrache, H. I.; Suter, R. M. *Biophys. J.* **1996**, 70, 1419.
- (30) Shelley, J. C.; Reeder, R. C. Manuscript in preparation.